Contents lists available at ScienceDirect

Arabian Journal of Chemistry

journal homepage: www.ksu.edu.sa

Preparation of biochar from pyrolysis of soybean straw at different pyrolysis temperature for cadmium removal from wastewater and pyrolysis gas investigation

Chao Lv [a], Peng Liu [b,*], Song Cheng [c,*]

[a] School of Coal Engineering, Shanxi Datong University, Datong, Shanxi 037009, China
[b] School of Vanadium and Titanium, Panzhihua University, Panzhihua 617000, China
[c] College of Chemistry and Chemical Engineering, Henan Polytechnic University, Jiaozuo 454003, China

ARTICLE INFO

Keywords:
Soybean straw
Pyrolysis
Cd^{2+}
Adsorption
Energy storage

ABSTRACT

The Cd^{2+} adsorption performance of biochar derived from soybean straw pyrolysis at 400–600 °C is investigated. Langmuir model can accurately describe the Cd^{2+} adsorption data with adsorption amount of 47.30 mg/g with pH=5. Cd^{2+} adsorption kinetic process could be analyzed using Pseudo-second-order. Biochar has large Cd^{2+} wastewater treatment volume, based on column adsorption experiment. The π-electrons play an important role in Cd^{2+} adsorption, based on adsorption mechanism analysis. Biochar has good stability after three cycles. Biochar also has good application potential used in lithium ion battery anode with specific capacity of 132 mA g^{-1}. Besides, pyrolysis gas is recycled in the preparation process of biochar with heating value of the 12.10 MJ/Nm^3. These results indicate that soybean straw waste is converted into sustainable adsorbent for Cd^{2+} wastewater treatment.

1. Introduction

Cadmium is a kind of the toxic heavy metal in the water ecosystem, which has caused a serious of the environmental problem to the humans (Nosuhi and Nezamzadeh-Ejhieh, 2017; Guo et al., 2024). The sources of cadmium-containing wastewater include the production process of metal mining, smelting, electrolysis, pesticide, medicine, inorganic pigment manufacturing, and electroplating. The cadmium can generate reactive oxygen species, which damage DNA structure and restrain DNA repair. Therefore, cadmium wastewater must be removed from wastewater to eliminate its environmental hazards to environment (Shafiof and Nezamzadeh-Ejhieh, 2020). The wastewater treatment methods include the chemical precipitation, membrane filtration, electrochemical treatment and adsorption (SalehA et al., 2013; Khani et al., 2010; Mehrali-Afjani and Nezamzadeh-Ejhieh, 2020). Adsorption is one of the widely used methods for cadmium wastewater treatment owe to the advantages of simple process and environment-friendly (Qin et al., 2023; Yuan et al., 2023). Therefore, adsorption technology is used as the effective method for cadmium wastewater treatment (Su et al., 2019; Guan et al., 2024). The biochar, activated carbon and zeolite molecular sieve are common adsorbents that are widely applied in wastewater treatment (Wang et al., 2024). However, the price of the common adsorbents is relatively expensive, resulted in the high cost of wastewater treatment. Therefore, preparation adsorbent with low-cost for large-scale wastewater treatment is urgent.

Biochar is a kind of the carbonaceous porous material, which belongs to the by-product of the biomass pyrolysis, and has promising potential in cadmium wastewater treatment (Huang et al., 2020; Fu et al., 2019). Yin et al. (2023) prepared the Pennisetum sp. straw biochar for cadmium wastewater treatment with the cadmium adsorption amount of the 53 mg/g (Yin et al., 2023). Yin et al. (2019) prepared the Pennisetum sp. straw biochars modified by $KMnO_4$ for cadmium wastewater purification with the adsorption amount of the 45.18 mg/g (Yin et al., 2019). Zhang et al.(2020) prepared the biochar derived from Agaricus bisporus substrate for cadmium removal from wastewater with the adsorption amount of the 64.80 mg/g (Zhang et al., 2020). Liu et al. (2020) prepared the blue algae-derived biochar, which has promising potential in cadmium wastewater removal with the adsorption amount of the 135.70 mg/g (Liu et al., 2021). Yang et al. (2023) prepared the novel MgO-modifed biochar derived from rice straw for cadmium wastewater removal with the adsorption amount of the 441.1 mg/g (Yang et al., 2023). Besides, biochar can be well generated with good stability after

* Corresponding authors.
E-mail addresses: tbagmo@126.com (P. Liu), chengsong@hpu.edu.cn (S. Cheng).

https://doi.org/10.1016/j.arabjc.2024.105946
Received 9 April 2024; Accepted 1 August 2024
Available online 2 August 2024

Table 1
Basis property of biochar produced at 400–600 °C.

Sample	BET (m^2/g)	C/%	H/%	N/%	O/%	H/C	O/C
B400 °C	50.17	69.81	2.25	0.54	27.4	0.032	0.39
B500 °C	126.32	75.14	2.13	0.92	21.81	0.028	0.29
B600 °C	190.56	76.33	1.96	0.78	20.93	0.026	0.27

Table 2
Kinetic parameters of Cd^{2+} adsorption on biochar produced at 400–600 °C.

Model	Parameters	B400 °C	B500 °C	B600 °C
Pseudo-first-order	qe.cal(mg/g)	20.84	24.92	27.97
	K_1(1/min)	0.01554	0.02217	0.0205
	R^2	0.8854	0.7373	0.8222
Pseudo-second-order	qe.cal(mg/L)	24.15	28.95	31.98
	K_2(g/mg.min)	0.000787	0.00082	0.00079
	R^2	0.9987	0.9975	0.9991
	h(mg/mg.min)	0.00036	0.00057	0.00064
Intraparticle diffusion	C(mg/g)	8.32	12.95	14.12
	K_3(mg/gmin$^{1/2}$)	0.653	0.657	0.746
	R^2	0.917	0.951	0.910

use using simple regeneration method. These above results demonstrate that biochar is the sustainability adsorbents for cadmium removal from wastewater.

The biochar obtained from biomass pyrolysis is much cheaper than that of the commercial activated carbon (Kearns et al., 2014). The typical price of commercial activated carbon is about US $ 2890/ton (Ng et al., 2003). Some literatures have reported the preparation cost of the biochar, which is about the US $ 246/ton (Ahmad et al., 2014) and US $ 51–386/ton (Meyer et al., 2011). Besides, the regeneration process of biochar is simple after use (Panahi et al., 2020). Therefore, biochar is the sustainable low-cost adsorbent for pollution wastewater treatment.

In this work, the soybean straw (SS) is the by-product of the soybean harvest. The SS is a kind of agricultural waste that is used for preparation of biochar using pyrolysis technology at different pyrolysis temperature for cadmium removal from wastewater. The physicochemical properties of biochar are analyzed. The cadmium adsorption capacity of the biochar prepared from different temperature is analyzed. The involved cadmium adsorption mechanisms on biochar are systematically investigated. The heating value and gases composition of the pyrolysis gas obtained from biochar preparation process are investigated. Besides, the possible of the biochar used in lithium-ion battery is also analyzed.

2. Materials and methods

2.1. Preparation of biochar

The SS is crushed with the particle size of about 840 μm. The 15 g SS is put in the resistance tube furnace, which is heated at 400–600 °C. The oxygen in the pyrolysis system is removed using the N_2 before starting experiment. Pyrolysis gas is collected from biochar preparation process, and purified for use. After that, the purification pyrolysis gas is named as the bio-gas. The biochar is the residue in resistance furnace after cooling. Biochar produced from the temperature of 400–600 °C is named as BY, and Y is temperature.

2.2. Adsorption experiment

The influence of initial pH on Cd^{2+} adsorption is analyzed at pH of 2–6. The 0.1 g biochar is put in the 100 mL Cd^{2+} solution at different Cd^{2+} concentrations, which is used to investigate adsorption isotherm of biochar. Residual Cd^{2+} concentration is detected using the atomic absorption spectrometer after reaching adsorption equilibrium. In the adsorption kinetic experiment, 0.1 g biochar is mixed in 100 mL Cd^{2+} solution (200 mg/L) to investigate adsorption capacity of biochar over time with pH of 5.

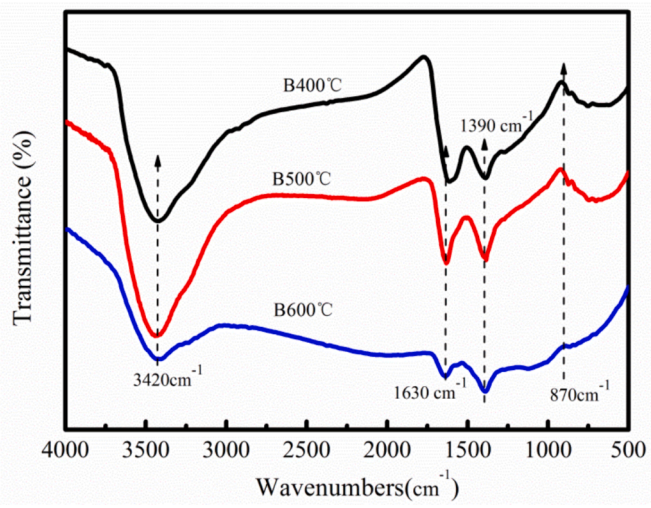

Fig. 1. Chemical functional groups of biochar produced at 400–600 °C.

Cd^{2+} adsorption amount (q_e or q_t) in above adsorption experiments are calculated as follows:

$$q_e = \frac{V(C_o - C_e)}{M} \quad (1)$$

$$q_t = \frac{V\ (C_o - C_t)}{M} \quad (2)$$

C_o is initial concentration. C_e and C_t are the equilibrium concentration and Cd^{2+} concentration over time, respectively. M is biochar mass. V is solution volume. Adsorption kinetics and isotherm models are listed in Tables 1-2 in the supporting material. The practical application of biochar is investigated in the column adsorption experiment.

3. Results and discussion

3.1. Physicochemical properties of biochar

Table 1 lists the basic property of biochar. Table 1 indicates that biochar has large C content at high temperature. This result indicates that biochar prepared from high temperature has high degree of aromaticity, indicating that high pyrolysis enhances the enrichment of C element. As Table 1 shown, the content of H and O decreases with increasing in pyrolysis temperature. Besides, O/C and H/C ratio also decrease with increasing in pyrolysis temperature. These results indicate that the biochar prepared from high temperature has large aromaticity and low polarity compared to low temperature (Sun et al., 2014).

Table1 also shows that biochar has large specific area with different temperature. The specific area of the biochar prepared form 600 °C is the largest than other pyrolysis temperature, indicating that temperature significantly influences the specific area of biochar. The pore and 2D annular structures are generally formed during the thermal decomposition of biomass as temperature increases.

Fig. 1 shows the chemical functional groups of the biochar. The —OH group is appeared at peaks of the 3420–3400 cm^{-1} (Fig. 1). All the samples have the prominent peak at around 1600 cm^{-1} band, which is the aromatic carbonyl/carboxyl C═O stretching. The oxygen-containing functional groups of biochar can bind with the metal ions, realizing the wastewater purification. The aliphatic chain of the CH_3— group is appeared at the peak of the 1380 cm^{-1} (Zhao et al., 2015). The biochar has the —CH group at round 870 cm^{-1} (Nowrouzi et al., 2017). However, the peaks intensity of the —OH and C═O group become weak at high temperature.

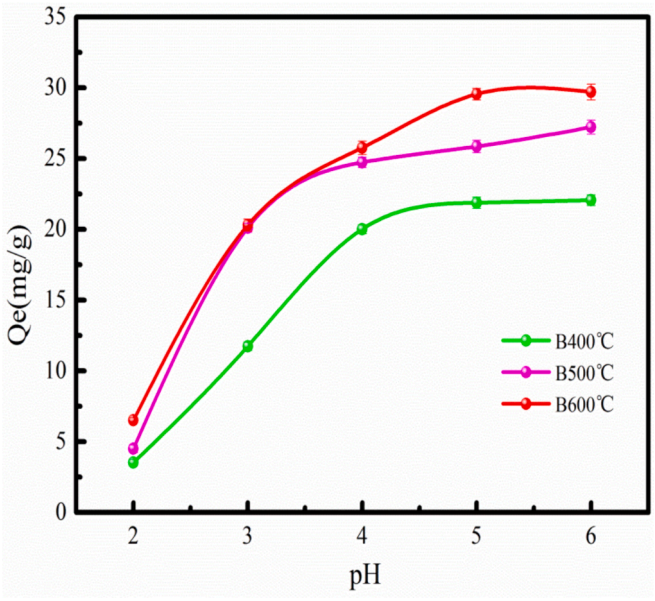

Fig. 2. Effect of pH on Cd^{2+} adsorption.

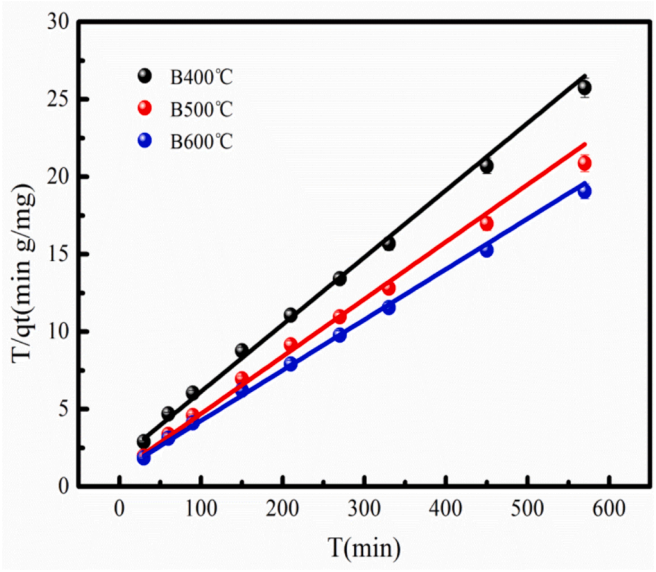

Fig. 3. Cd^{2+} adsorption data fitting the pseudo-second-order kinetic model.

3.2. Influence of pH

Fig. 2 shows the influence of initial pH on Cd^{2+} adsorption. Fig. 2 indicates that the pH value significantly influences the adsorption performance of the biochar. The Cd^{2+} adsorption amount is low at pH=2–3. In a word, the Cd^{2+} adsorption on biochar is hindered (Omrani and Nezamzadeh-Ejhieh, 2020). However, the H^+ concentration generally decreases with increasing in pH value. Therefore, Cd^{2+} adsorption capability generally increases with increasing in pH value. However, the precipitation is formed in the Cd^{2+} solution at pH>7.34 (Cheng et al., 2021). The solution with a certain of H^+ concentration will contribute to Cd^{2+} adsorption on biochar. Besides, the precipitation of the Cd^{2+} can be hindered. Therefore, Cd^{2+} adsorption with the pH of 5 is feasible.

3.3. Adsorption kinetics

Adsorption kinetics models such as pseudo-first-order, pseudo-second-order and intraparticle diffusion model are used to describe the adsorption kinetics process (Yang et al., 2021). The fitting results of the Cd^{2+} adsorption data fitting the above adsorption kinetics models are listed in Table 2. As Table 2 shown, the biochar prepared from high temperature has large Cd^{2+} adsorption amount, which is larger than that low temperature. The pseudo-second-order model has the largest correlation coefficient (R^2) than the pseudo-first-order and intraparticle diffusion models. Therefore, Cd^{2+} adsorption on biochar analyzed by the pseudo-second-order model is feasible. Besides, Cd^{2+} adsorption on biochar is influenced by chemisorption. Fig. 3 shows the fitting results using pseudo-second-order model. The intraparticle diffusion model is also used to fit Cd^{2+} adsorption data (Fig. S1). As Fig. S1 shown, the intercept of the fitting curve is not zero, indicating that the mass transfer rate of Cd^{2+} adsorption on biochar is different in initial and final adsorption stages. The fitting C values of biochar are in the range of the 8.32–14.12. This result indicates that rate-limiting step of Cd^{2+} adsorption on biochar is influenced by the intraparticle diffusion.

Table 3
Adsorption isotherm parameters of Cd^{2+} adsorption on biochar produced at 400–600 °C.

Isotherms	Parameters	B400 °C	B500 °C	B600 °C
Langmuir	Q_0(mg/g)	33.91	39.18	47.30
	K_L(L/mg)	0.0117	0.0155	0.0112
	R^2	0.9935	0.9914	0.9967
Freundlich	K_F((mg/g).(L/mg)$^{1/n}$)	5.6279	8.7501	6.9065
	1/n	0.2713	0.3391	0.2925
	R^2	0.9742	0.9579	0.9124

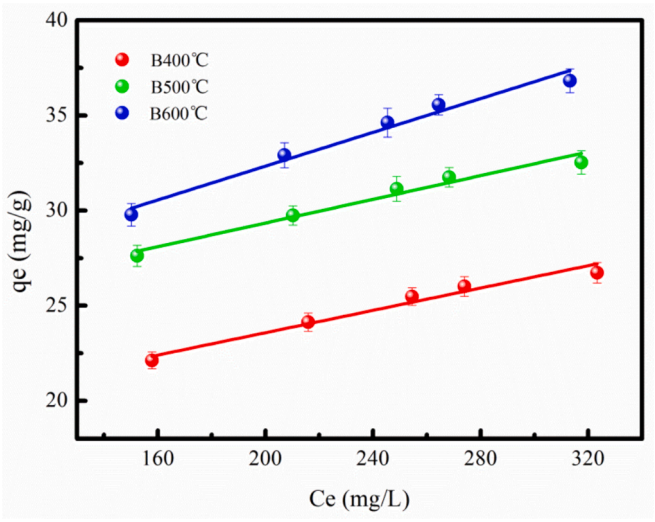

Fig. 4. Cd^{2+}adsorption data fitting the Langmuir model.

3.4. Adsorption isotherms

Langmuir and Freundlich isotherm models are used to analyze the Cd^{2+} adsorption process. The Cd^{2+} adsorption parameters are calculated from adsorption isotherm data fitting adsorption isotherm model, which are listed in Table 3. Langmuir isotherm model better fits Cd^{2+} + adsorption data compared to the Freundlich isotherm owe to large coefficients R^2 (Table 3). The Cd^{2+} adsorption amount of biochar produced at large temperature is large compared to biochar produced at low temperature, based on fitting results in Table 3. It might be explained that the biochar produced at large temperature has high BET surface area that contributes to Cd^{2+} adsorption. In addition, biochar has abundant surface chemical functional group and mineral component, which also contribute to Cd^{2+} removal. The fitting curve of the Cd^{2+}

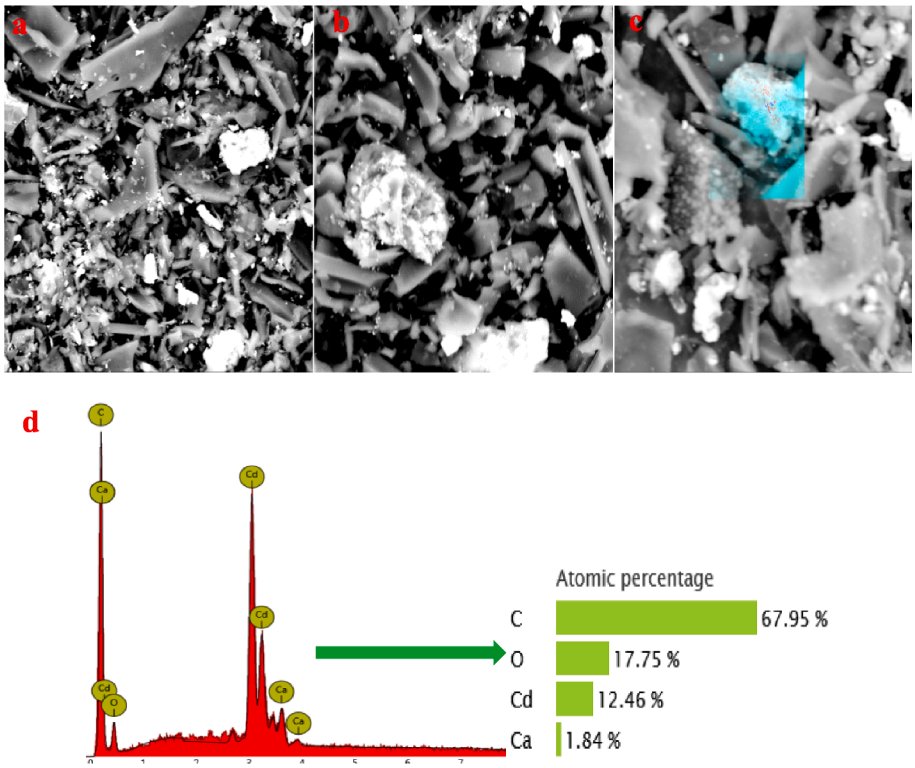

Fig. 5. SEM-EDX images of B600 °C loaded Cd^{2+} (a-d).

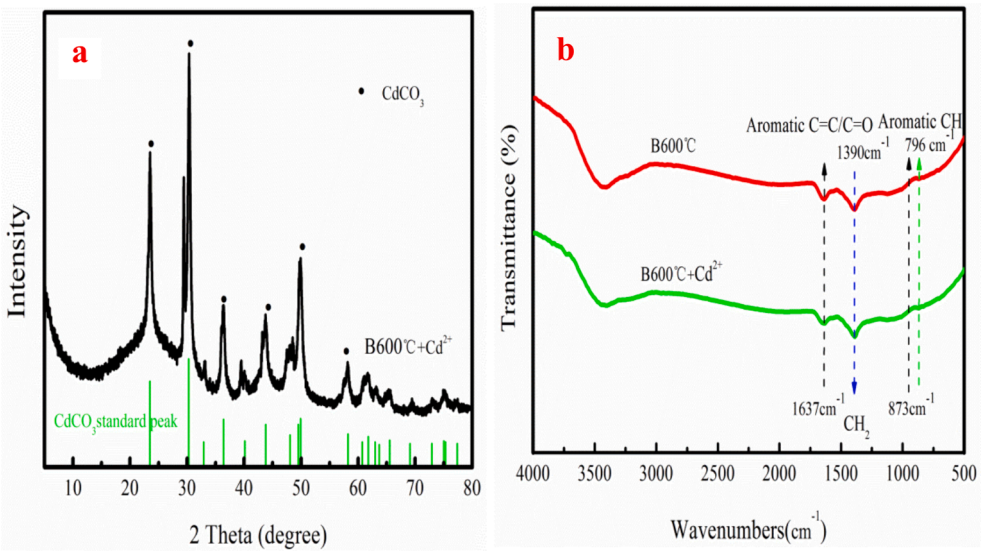

Fig. 6. XRD pattern of B600 °C after adsorption Cd^{2+} (a), FTIR of B600 °C before and after adsorption Cd^{2+} (b).

adsorption on biochar using Langmuir model is shown in Fig. 4. The Cd^{2+} adsorption capability of various of the biochar is summarized in Table S3. The biochar produced from SS has large Cd^{2+} adsorption capability compared to other biochar, demonstrating that SS biochar might be acted as an efficient adsorbent for Cd^{2+} removal from wastewater. B600 °C is acted as the candidate for further utilization and study due to large Cd^{2+} adsorption amount.

3.5. Recyclability of biochar

The reusability can be employed as an important parameter to investigate the practical application of biochar. The recyclability result of biochar is shown in Fig. S2. The Cd^{2+} adsorption amount of regenerated biochar decreases as cycle increases (Fig. S2). The Cd^{2+} adsorption capability is 22.91 mg/g at third cycle. The reason might be that biochar loses part of adsorption sites after regeneration, resulted in the decrease of Cd^{2+} adsorption amount (Herath et al., 2020). This result proves that biochar might be used as the recyclable adsorbent for Cd^{2+} removal from wastewater.

3.6. Adsorption mechanism

Fig. 5 shows the SEM-EDX images of B600 °C after Cd^{2+} adsorption. After Cd^{2+} adsorption, the surface of B600 °C appears grayish white

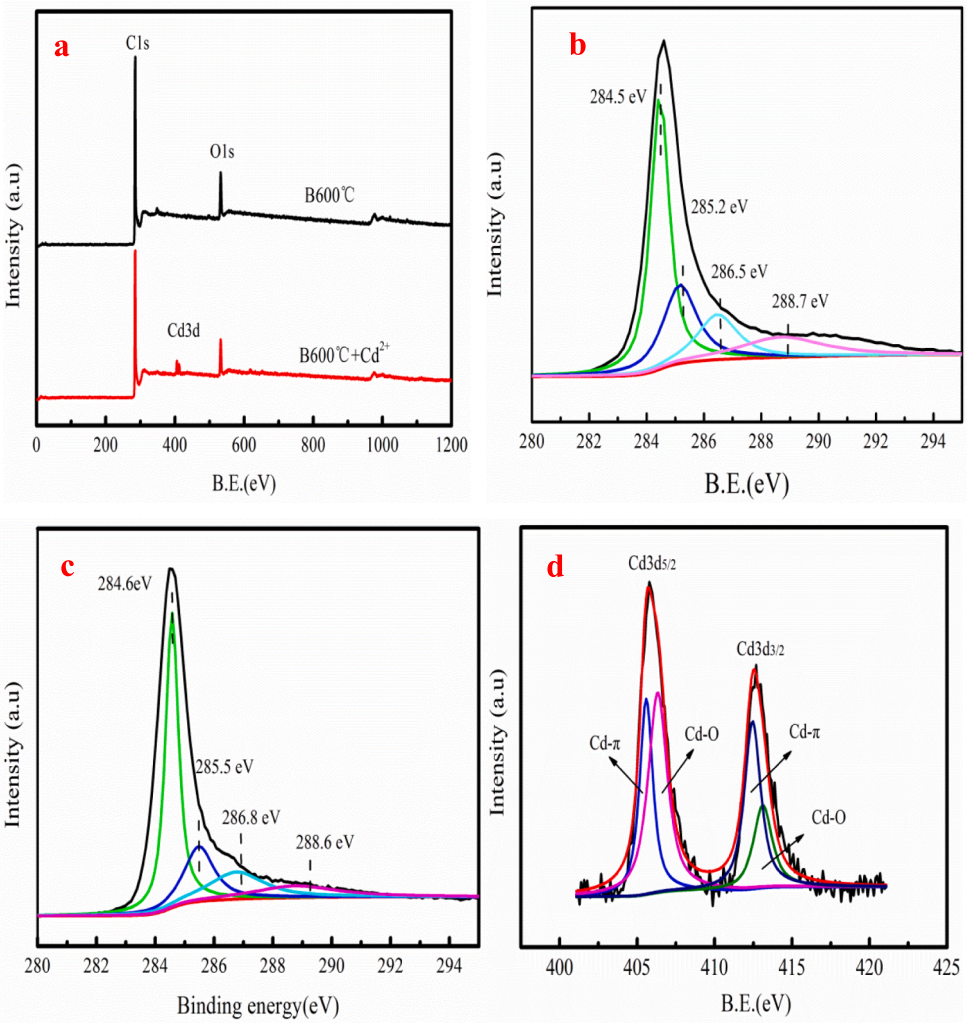

Fig. 7. The wide scan XPS spectrum (a) and C 1 s XPS spectra before and after Cd^{2+} adsorption (b-c), XPS survey spectra along with the spectra of Cd3d (d) after adsorption.

particles, which are carbon, oxygen, calcium and cadmium, based on EDX analysis. This result proves that Cd^{2+} is adsorbed by B600 °C. XRD is used to analyze the adsorption status of Cd^{2+} on B600 °C. Fig. 6a shows that $CdCO_3$ is appeared on B600 after Cd^{2+} adsorption (Wang et al., 2015; Xu et al., 2013). The existence of the $CdCO_3$ indicates that the carbonate in B600 °C might react with Cd^{2+} to form the $CdCO_3$; which is one of the Cd^{2+} removal methods.

B600 °C before and after adsorption Cd^{2+} is analyzed by the FTIR spectrum (Fig. 6b). As Fig. 6b shown, the aromatic structure of —CH of the B600 °C is appeared at peak of the 874–796 cm^{-1}. The —CH group is a kind of the weak cation-π binding agent, which could bind with the Cd^{2+}, resulted in the formation of the Cd-π (Xie et al., 2014). The peak intensity of 874–796 cm^{-1} is weaker after adsorption compared to before Cd^{2+} adsorption, resulted in the formation of the Cd-π on B600 °C after Cd^{2+} adsorption. The CH_2 group is appeared at peak the 1390 cm^{-1}. However, the peak location has changed after adsorption. Besides, peak position of C═C/C═O group also has changed after adsorption. The above results demonstrate that it is existence of the Cd^{2+}-π interaction during adsorption process owe to high graphitization degree of the B600 °C.

B600 °C also has inorganic salt ions (magnesium, calcium and potassium ions). Therefore, it is existence of ion exchange between Cd^{2+} and inorganic salt ions during adsorption process. Therefore, ion exchange could also realize Cd^{2+} removal from wastewater. The Mg^{2+}, Ca^{2+} and K^{+} concentrations in the Cd^{2+} adsorption process are 2.94, 2.68 and 0.35 mg/L, respectively, demonstrating that ion exchange occurs during Cd^{2+} adsorption process.

XPS spectrum is used to investigate Cd^{2+} adsorption behavior on biochar. As Fig. 7 shown, O 1 s spectrum has three peaks. The C═O, C—O and O—C═O groups are corresponded to the peaks of the 531.46, 532.54 and 533.69 eV, respectively (Wang et al., 2018). However, the peak area and binding energy of C═O, C—O and O—C═O groups change after Cd^{2+} adsorption. Peak area of C—O and O—C═O decreases from 41.76 % and 29.02 % to 36.49 % and 23.21 % after Cd^{2+} adsorption, respectively. The analysis result shows that the oxygen-containing functional groups involve into Cd^{2+} adsorption (Zhang et al., 2017). The spectrum of Cd3d is used to analyze the binding energy of Cd^{2+} adsorption on biochar, which have four peaks. The analysis result indicates that the existence form of the cadmium is presented as Cd^{2+} (43.78 %) and Cd-O (56.22 %).

3.7. Column adsorption experiment

The practical application of the B600 °C is investigated in the column adsorption experiment. The Cd^{2+} solution with 1 mg/L is employed as simulated wastewater to explore column adsorption performance of B600 °C. Single bed volume (BV) of column adsorption is 20 mL. Fig. S3 shows the corresponding breakthrough curve. As Fig. S3 shown, the effective treatment volume of Cd^{2+} is 820 mL. This result indicates that B600 °C has potential in the long-term application.

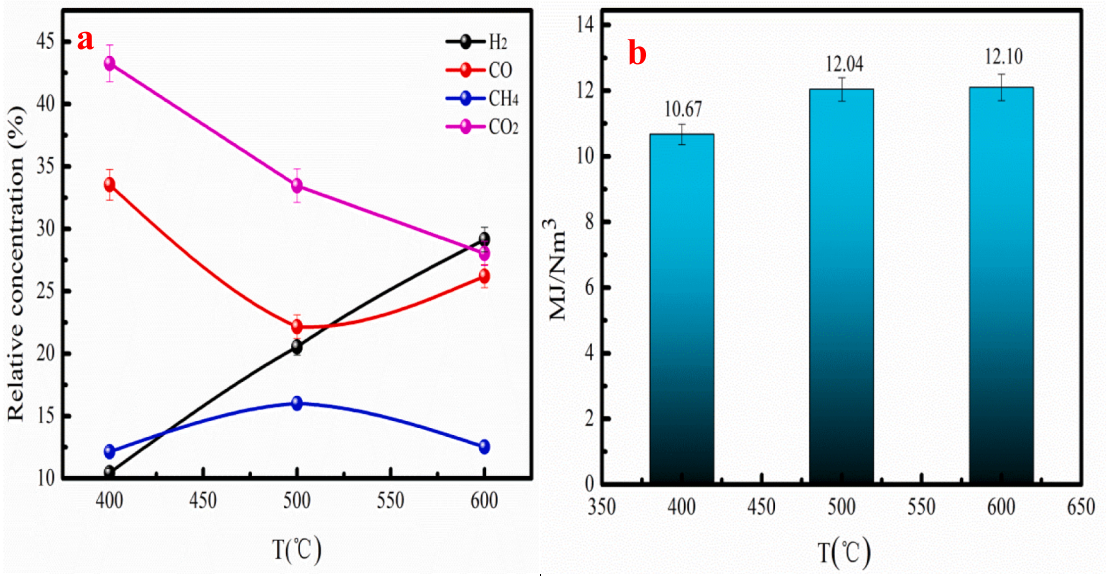

Fig. 8. The composition (a) and lower heating value (LHV) (b) of bio-gas produced at 400–600 °C.

3.8. Application biochar in energy storage

The rate performance of B600 °C is used to investigate the energy storage potential used in lithium ion batteries at different current densities of 50–2000 mA g^{-1} (Fig. S4). The initial charge and discharge is 41.59 %, based on analysis result. The specific capacity of B600 °C at 50–2000 mA g^{-1} is 132, 102, 82, 53, 32, 19 and 159 mA g^{-1}, respectively. Table 1 shows that the N content of B600 °C is large. This result indicates that N of the B600 °C can form pyridine- and pyrrolic-type nitrogen-doped atoms. The formed nitrogen-containing structure of the biochar contributes to lithium storage, and improves the specific capacity, based on theoretical calculation. These structural advantages greatly improve the electrochemical performance of B600 °C. Therefore, B600 °C shows promising application potential in energy storage.

3.9. Pyrolysis gas investigation

The composition and lower heating value (LHV) of bio-gas are analyzed to investigate the application potential of the pyrolysis gas. The gases composition and LHV of bio-gas are presented in the Fig. 8. As shown in Fig. 8a, the bio-gas has high percentage of the CO_2 at 400–500 °C. However, the CO_2 percentage of the bio-gas is decrease with increasing in temperature. This result demonstrates that the generation process of the CO_2 is restrained at high temperature. The CO content of bio-gas is decrease before 500 °C. However, the CO content of bio-gas increases after 500 °C, proving that high temperature contributes to CO generation. Fig. 8a indicates that bio-gas has low H_2 content at low temperature, and high H_2 content at high temperature, indicating that low temperature doesn't contribute to the production of H_2. The CH_4 content of the bio-gas is decrease after 500 °C with content of 16.02 %. Fig. 8b indicates that the LHV of bio-gas is increase as temperature increases with the maximum LHV of the 12.10 MJ/Nm^3. The bio-gas has large LHV, which has promising application potential in industry.

4. Conclusion

The biochar is prepared from soybean straw pyrolysis at different pyrolysis temperature, which has large Cd^{2+} adsorption amount. The physicochemical properties such as pore structure and chemical functional groups of the biochar are investigated. The pseudo-second-order model can be used to describe Cd^{2+} adsorption kinetic process. Cd^{2+} adsorption amount is 47.30 mg/g based on Langmuir model calculation. Cd^{2+}-π interaction has significantly influenced on Cd^{2+} adsorption process, based on the adsorption mechanism analysis. Biochar has good recyclability, which still has the high Cd^{2+} adsorption capacity after regeneration. The column adsorption analysis results indicate that biochar has the great potential in Cd^{2+} wastewater treatment. Bio-gas obtained from pyrolysis process has large LHV with 12.10 MJ/Nm^3. Besides, biochar has the potential of the energy storage with the specific capacity of 132mA g^{-1}.

Funding

The authors would like to express their gratitude to the Specialized Research Fund for the Fundamental Research Program of Shanxi Province(202403021211071), Science and Technology Plan Project of Datong City (2020139), Basic research project of Shanxi Datong University(2022Q36), Natural Science Foundation of Henan Province (232300420298), Panzhihua Directed Science and Technology Planning Projects (2022ZD-G-4), and Scientific Research Fund of Panzhihua University (XJ2022001301) for financial support.

Ethical approval.

Not applicable.

CRediT authorship contribution statement

Chao Lv: Writing – original draft, Investigation, Formal analysis, Conceptualization. **Peng Liu:** Writing – original draft, Supervision, Funding acquisition, Formal analysis. **Song Cheng:** Writing – original draft, Funding acquisition, Formal analysis, Data curation, Conceptualization.

Declaration of competing interest

The authors declare that they have no known competing financial interests or personal relationships that could have appeared to influence the work reported in this paper.

Appendix A. Supplementary data

Supplementary data to this article can be found online at https://doi.org/10.1016/j.arabjc.2024.105946.

References

Ahmad, M., Rajapaksha, A.U., Lim, J.E., Ming, Z., Bolan, N., Mohan, D., Vithanage, M., Sang, S.L., Yong, S.O., 2014. Biochar as a sorbent for contaminant management in soil and water: a review. Chemosphere 99, 19–33.

Cheng, S., Liu, Y., Xing, B., Qin, X., Zhang, C., Xia, H., 2021. Lead and cadmium clean removal from wastewater by sustainable biochar derived from poplar saw dust. J. Clean. Prod. 314, 128074.

Fu, M.M., Mo, C.H., Li, H., Zhang, Y.N., Huang, W.X., Wong, M.H., 2019. Comparison of physicochemical properties of biochars and hydrochars produced from food wastes. J. Clean. Prod. 236, 117637.

Guan, D., Zhao, J., Wang, Y., Fu, Z., Zhang, D., Zhang, H., Xie, J., Sun, Y., Zhu, J., Wang, D., 2024. A critical review on sustainable management and resource utilization of digestate. Process Saf. Environ. Prot. 183, 339–354.

Guo, H., Cheng, S., Xing, B., Meng, M., Feng, L., Nie, Y., Zhang, C., 2024. Preparation of three kinds of efficient sludge-derived adsorbents for metal ions and organic wastewater purification. Arab. J. Chem. 17, 105671.

Herath, A., Layne, C.A., Perez, F., Hassan, E.B., Mlsna, T.E., 2020. KOH-activated high surface area douglas fir biochar for adsorbing aqueous Cr(VI), Pb(II) and Cd(II). Chemosphere 269, 128409.

F. Huang, K. Li, R.R. Wu, Y.J. Yan, R.B. Xiao. (2020) Insight into the Cd^{2+} biosorption by viable Bacillus cereus RC-1 immobilized on different biochars: Roles of bacterial cell and biochar matrix, Journal of Cleaner Production, 272 (2020) Insight into the Cd^{2+} biosorption by viable Bacillus cereus RC-1 immobilized on different biochars: Roles of bacterial cell and biochar matrix.

Kearns, J.P., Wellborn, L.S., Summers, R.S., Knappe, D., 2014. 2,4-D adsorption to biochars: Effect of preparation conditions on equilibrium adsorption capacity and comparison with commercial activated carbon literature data. Water Res. 62, 20–28.

Khani, H., Rofouei, M.K., Arab, P., Gupta, V.K., Vafaei, Z., 2010. Multi-walled carbon nanotubes-ionic liquid-carbon paste electrode as a super selectivity sensor: application to potentiometric monitoring of mercury ion(II). J. Hazard. Mater. 183, 402–409.

Liu, P., Rao, D., Zou, L., Teng, Y., Yu, H., 2021. Capacity and potential mechanisms of Cd (II) adsorption from aqueous solution by blue algae-derived biochars. Sci. Total Environ. 767, 145447.

Mehrali-Afjani, M., Nezamzadeh-Ejhieh, A., 2020. Efficient solid amino acid-clinoptilolite nanoparticles adsorbent for Mn(II) removal: a comprehensive study on designing the experiments, thermodynamic and kinetic aspects. Solid State Sci. 101, 106124.

Meyer, S., Glaser, B., Quicker, P., 2011. Technical, economical, and climate-related aspects of biochar production technologies: a literature review. Environ. Sci. Technol. 45, 9473–9483.

Ng, C., Marshall, W.E., Rao, R.M., Bansode, R.R., Losso, J.N., 2003. Activated carbon from pecan shell: process description and economic analysis. Ind. Crop. Prod. 209–217.

Nosuhi, M., Nezamzadeh-Ejhieh, A., 2017. High catalytic activity of Fe(II)-clinoptilolite nanoparticales for indirect voltammetric determination of dichromate: experimental design by response surface methodology (RSM). Electrochim. Acta 223, 47–62.

Nowrouzi, M., Behin, J., Younesi, H., Bahramifar, N., Charpentier, P.A., Rohani, S., 2017. An enhanced counter-current approach towards activated carbon from waste tissue with zero liquid discharge. Chem. Eng. J. 934–944.

Omrani, N., Nezamzadeh-Ejhieh, A., 2020. Focus on scavengers' effects and GC-MASS analysis of photodegradation intermediates of sulfasalazine by Cu_2O/CdS nanocomposite. Sep. Purif. Technol. 235, 116228.

Panahi, H.K.S., Dehhaghi, M., Ok, Y.S., Nizami, A.-S., Khoshnevisan, B., Mussatto, S.I., Aghbashlo, M., Tabatabaei, M., Lam, S.S., 2020. A comprehensive review of engineered biochar: production, characteristics, and environmental applications. J. Clean. Prod. 270, 122462.

Qin, X., Cheng, S., Xing, B., Qu, X., Shi, C., Meng, W., Zhang, C., Xia, H., 2023. Preparation of pyrolysis products by catalytic pyrolysis of poplar: application of biochar in antibiotic wastewater treatment. Chemosphere 338, 139519.

SalehA, T.A., Gupta, V.K., Al-Saadi, A.A., 2013. Adsorption of lead ions from aqueous solution using porous carbon derived from rubber tires: experimental and computational study. J. Colloid Interface Sci. 396, 264–269.

Shafiof, M.a.S., Nezamzadeh-Ejhieh, A., 2020. A comprehensive study on the removal of Cd(II) from aqueous solution on a novel pentetic acid-clinoptilolite nanoparticles adsorbent: experimental design, kinetic and thermodynamic aspects. Solid State Sci. 99.

Su, S.L., Yek, P., Yong, S.O., Chi, C.C., Peng, W., 2019. Engineering pyrolysis biochar via single-step microwave steam activation for hazardous landfill leachate treatment. J. Hazard. Mater. 390, 121649.

Sun, Y., Gao, B., Yao, Y., Fang, J., Zhang, M., Zhou, Y., Chen, H., Yang, L., 2014. Effects of feedstock type, production method, and pyrolysis temperature on biochar and hydrochar properties. Chem. Eng. J. 240, 574–578.

Wang, R.Z., Huang, D.L., Liu, Y.G., Zhang, C., Lai, C., Zeng, G.M., Cheng, M., Gong, X.M., Wan, J., Luo, H., 2018. Investigating the adsorption behavior and the relative distribution of Cd^{2+} sorption mechanisms on biochars by different feedstock. Bioresour. Technol. 261, 265–271.

Wang, Z., Liu, G., Zheng, H., Li, F., Ngo, H.H., Guo, W., Liu, C., Chen, L., Xing, B., 2015. Investigating the mechanisms of biochar's removal of lead from solution. Bioresour Technol 177, 308–317.

Wang, Y., Zhao, J., Fu, Z., Guan, D., Zhang, D., Zhang, H., Zhang, Q., Xie, J., Sun, Y., Wang, D., 2024. Innovative overview of the occurrence, aging characteristics, and ecological toxicity of microplastics in environmental media. Environ. Pollut. 346, 123623.

Xie, M., Chen, W., Xu, Z., Zheng, S., Zhu, D., 2014. Adsorption of sulfonamides to demineralized pine wood biochars prepared under different thermochemical conditions. Environ. Pollut. 186, 187–194.

Xu, X., Cao, X., Ling, Z., Wang, H., Yu, H., Gao, B., 2013. Removal of Cu, Zn, and Cd from aqueous solutions by the dairy manure-derived biochar. Environ. Sci. Pollut. Res. Int. 20, 358–368.

Yang, K., Cheng, Z., Luo, W., Guo, B., Zhang, B., Zhang, Y., 2023. Adsorption performance and mechanisms of MgO-modified palygorskite/biochar composite for aqueous Cd (II): experiments and theoretical calculation. Appl. Surf. Sci. 638, 157965.

Yang, T., Xu, Y., Huang, Q., Sun, Y., Zhao, L., 2021. Adsorption characteristics and the removal mechanism of two novel Fe-Zn composite modified biochar for Cd(II) in water. Bioresour. Technol. 333, 125078.

Yin, G., Bi, L., Song, X., Luo, H., Ji, P., Lin, Q., Liu, Q., Tang, G., 2019. Adsorption of Cd (II) from aqueous solution by Pennisetum sp. straw biochars derived from different modification methods. Environ. Sci. Pollut. Res. 26, 2318.

Yin, G., Chen, X., Sarkar, B., Bolan, N.S., Wei, T., Zhou, H., Wang, H., 2023. Co-adsorption mechanisms of Cd(II) and As(III) by an Fe-Mn binary oxide biochar in aqueous solution. Chem. Eng. J. 466, 143199.

Yuan, Q., Zhang, H., Qin, C., Zhang, H., Wang, D., Zhang, Q., Zhang, D., Zhao, J., 2023. Impact of emerging pollutant florfenicol on enhanced biological phosphorus removal process: Focus on reactor performance and related mechanisms. Sci. Total Environ. 859, 160316.

Zhang, G., Liu, N., Luo, Y., Zhang, H., Cheng, H., 2020. Efficient removal of Cu(II), Zn(II), and Cd(II) from aqueous solutions by a mineral-rich biochar derived from a spent mushroom (Agaricus bisporus) substrate. Materials 14, 35.

Zhang, C., Shan, B., Tang, W., Zhu, Y., 2017. Comparison of cadmium and lead sorption by Phyllostachys pubescens biochar produced under a low-oxygen pyrolysis atmosphere. Bioresour. Technol. 238, 352–360.

Zhao, Y., Feng, D., Yu, Z., Huang, Y., Sun, S., 2015. Effect of pyrolysis temperature on char structure and chemical speciation of alkali and alkaline earth metallic species in biochar. Fuel Process. Technol. 141, 54–60.